

# Field Quality Measurements of the LQXB Inner Triplet Quadrupoles for LHC

G.V. Velev, R. Bossert, R. Carcagno, J. DiMarco, S. Feher, H. Glass, V.V. Kashikhin, J. Kerby, M. Lamm, A. Makulski, A. Nobrega, J. Nogiec, D. Orris, T. Peterson, R. Rabehl, P. Schlabach, J. Strait, C. Sylvester, M. Tartaglia, J.C. Tompkins, A.V. Zlobin

**Abstract** As a part of the USLHC program, Fermilab is building half of the inner triplet quadrupole magnets for the LHC. Two identical quadrupoles (MQXB) with a dipole corrector between them in a single cryogenic unit (LQXB) comprise the Q2 optical element of the final focus triplets in the interaction regions. The 5.5 m long MQXB have a 70 mm aperture and operate in superfluid helium at 1.9 K with a peak field gradient of 215 T/m. Manufacturing of the 18 magnets is in an advanced stage. A program of magnetic field quality measurements of the magnets is performed at room temperature during magnet fabrication as well as at superfluid helium temperature during the cold qualification of each magnet. Results of the measurements are summarized in this paper.

**Index Terms** magnetic fields, quadrupole, superconductivity

## I. INTRODUCTION

TO meet the high luminosity design specification ( $10^{34}$  cm<sup>-2</sup>s<sup>-1</sup>) for the future Large Hadron Collider (LHC), special high gradient quadrupoles for the interaction regions are required [1]. These magnets, arranged as the final focus triplet (Q1, Q2, Q3, shown on the schematic in Fig.1), have to provide a maximum operating gradient of 215 T/m at 1.9K in superfluid helium over a 70 mm coil bore due to a large variation of the  $\beta$ -function of the beam in the interaction regions. Half of these superconducting low-beta quadrupoles (MQXB) for the interaction regions are provided by Fermilab. The other half (MQXBA) were produced by KEK [2] and the final assembly, including the cryostating of all the magnets, is ongoing at Fermilab. To date 15 of the cold MQXB masses have been built. Fourteen of them (MQXB01-12, 14,15), together with the corresponding correctors (MCBX), were selected for the assembly of the first five LQXB01-06 cryogenic units. Six of LQXB01-06 have been cold tested, LQXB07 is currently undergoing testing.

The MQXB design, developed in collaboration with LBNL and BNL, is based on four two-layered coils connected in series. The coils are surrounded by stainless steel collars and

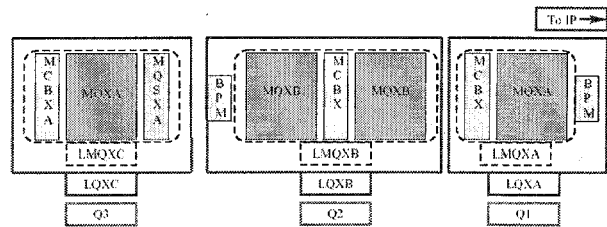


Fig. 1 Schematic of the LHC focusing inner triplet system. The LQXB magnet is the middle element in the triplet and consists two MQXB quadrupoles.

iron yoked laminations. Details of the MQXB design, changes and improvements during the initial test model program, are reported elsewhere [3-6].

In this paper we present the results of the warm field production measurements of MQXB01-15 in collared and yoked stages. The result from cold magnetic measurements are summarized and discussed as well.

## II. MEASUREMENT SYSTEMS

Magnetic measurements were performed at the Fermilab Magnet Test Facility. The field harmonics are measured with a horizontal drive rotating coil system which is described below. Integral strength measurement is based on a Single Stretched Wire (SSW) system described in [7].

### A. Measurement stands

Two similar horizontal stands were built for performing magnetic measurements. The stands utilize horizontal translation devices for positioning the rotating coil in the desired z-position in a magnet. For in-process testing of the individual MQXB cold mass, a measurement stand with a 7.5 m stroke was used and for the final quality assurance magnetic measurements performed at superfluid (1.9K) temperature, a stand with an 11.5 m stroke was used. The schematic sketch of the stands is presented in fig.2.

The rotating probe is connected to the drive system by a long drive shaft that is assembled from 1.5 m long sections. Included in each section is a bearing assembly and a flexible coupling. This shaft assembly is used to transfer the rotation from the precisely controlled stepper motor to the probe. A 10:1 ratio gear box is utilized as part of the probe drive

Manuscript received October 5, 2004. Work supported by the U.S. Department of Energy.

All authors are with Fermilab, P.O. Box 500, Batavia, IL 60510, USA, (e-mail: [velev@fnal.gov](mailto:velev@fnal.gov); phone: 630-840-2203; fax: 630-840-2383).

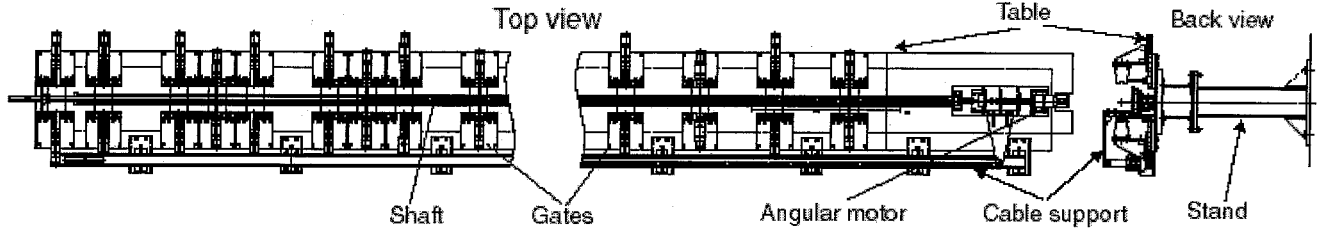


Fig. 2. Schematic view of the measurement stand

assembly to smooth out the angular steps from the motor. The longitudinal insertion of the probe is achieved with the use of the motor and belt driven horizontal translation device, in conjunction with the cycling (open/close) of a set of support gates. The gates support the drive shaft against gravity, and they are spaced on the table, relative to the position of a flexible coupling and bearing in such a way as to have alternate gates in the open position at all times. At any given time, 50 percent of the gates are open while the rest are supporting the shaft assembly. The gates are controlled by photo-eyes and cycle open/close via pneumatic cylinders when a bearing assembly or flexible coupling which are larger in diameter than the shaft, approach the gate.

### B. Measurement probes and DAQ system

Similar probes were utilized for the warm and cold magnetic measurements. They have a tangential winding for determination of higher order harmonics as well as two dipole and two quadrupole windings sensitive to the lowest order field components. The geometry of the probes is selected in a way that allows a bucking of the large low order field components in the tangential winding signal. The warm measurements, for quality control during cold mass production, are made with a coil of 31.8 mm nominal radius and of 0.91 m length. For the cold measurements two different probes were exploited. The integral harmonics are obtained using a 7.1 m long rotating coil with 41 mm nominal diameter assembled from three independent probes connected in series. In addition to the integral measurements a DC cold scan was done with an 81 cm long probe of 39.2 mm nominal diameter.

The DAQ system is based on five Metrolab PDIs (model 5035) reading the coil winding voltages. An HP3458 DVM is used to monitor the magnet current. PDIs and DVM are triggered by an angular encoder directly connected to the probe shaft and it synchronizes the simultaneous measurements of field and current. To center the probe in the magnet a feed down technique of the off-centered quadrupole to the dipole field is applied

## III. FIELD ANALYSIS

All results are expressed according to the convention that the field is represented in terms of harmonics coefficients defined in a series expansion given by

$$B_y + iB_x = B_2 10^{-4} \sum_{n=1}^{\infty} (b_n + ia_n) \left( \frac{x+iy}{r_0} \right)^{n-1}$$

where  $B_x$  and  $B_y$  are the field components in the Cartesian coordinates,  $b_n$  and  $a_n$  are the  $2n$ -pole normal and skew coefficients at the reference radius  $r_0$  of 17 mm chosen for LHC ( $b_2 = 10^4$ ). The coordinate system is defined in [8].

### A. Results of the warm measurements

In the process of production of every MQXB magnet, two measurements are performed to ensure magnet quality. In the first one, an integral z-scan of the collared coil is executed. This measurement checks the quality of the coil assembly due to the collaring process. The second z-scan follows the yoking process. The rotating coil probe is placed at the same z-positions as for the collared coil measurements. This allows us to determine harmonic changes due to the addition of the yoke and the welding process.

Fig. 3 shows the harmonics up to the dodecapole for the MQXB01-15 production cold masses (open and filled triangles for normal and skew harmonics respectively). The values are compared to the average of the last five magnets from the model program (open and filled circles, the error bars represent one sigma deviation) [2,8] and to the full scale prototype (open and filled diamonds) [9]. An acceptable but systematic deviation from the average harmonics of short model magnet tests is observed in the normal dodecapole for the first three cold masses MQXB01-03 (see fig.3 bottom right corner).

The similar result for  $b_6$  is obtained for the yoked cold masses. The correlation between dodecapole measured before and after yoking is shown in fig.4. The solid line corresponds to the case of no change in  $b_6$ . In spite of the dodecapole  $b_6$

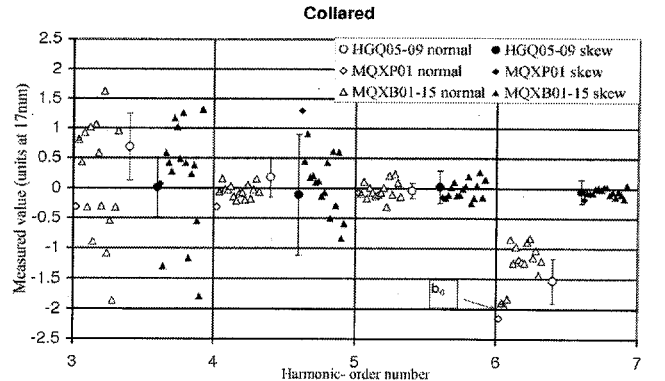


Fig. 3. Measured collared coil harmonics in the body of MQXB01 through MQXB15. The open and filled circles represent the average harmonics derived from the model magnet program. The error bars are one sigma. The arrow points at a systematically larger dodecapole for the prototype and the first three production cold masses.

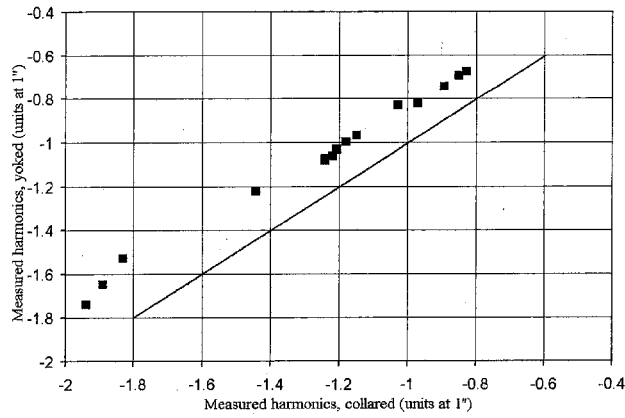


Fig. 4. Correlation between the normal dodecapole before and after process of cold mass yoking.

decreases of an average of 0.2 units after yoking a performed accelerator simulation pointed to the possibility that in some configurations  $b_6$  could be too large to be compensated with the available corrector strength. An effort was made in the production to decrease the normal dodecapole deviation. The result of the field calculation was implemented first in the MQXB04 cold mass. A new shim pattern in the coils was applied. Measurements of the collared coil showed a change of 1.2 units in  $b_6$ , somewhat larger than the expected 0.8 units from the calculation. After additional tuning the coil shimming pattern was fixed for MQXB05 and the following cold masses. In detail the correction procedure is described in [10,11].

### B. Cold measurements

The final quality assurance magnetic measurements were performed at superfluid helium temperature ( $\sim 1.9\text{K}$ ) on the MQXB cold masses assembled in cryogenic units LQXB01-06 (except for rejected LQXB02 assembly due to limited quench performance of MQXB04 [12]). The integral field harmonics at 11.9 kA (215 T/m), up to order 10, are presented in Fig 5. They are compared with the reference values v3.2 [3] that were derived from the latter stage of the model magnet program. The errors assigned to the reference means (see Fig.5 points with error bars), correspond to  $\delta(b_n, a_n) = d(b_n, a_n) + 3\sigma(b_n, a_n)$ , where  $d$  and  $\sigma$  are the uncertainties in mean and

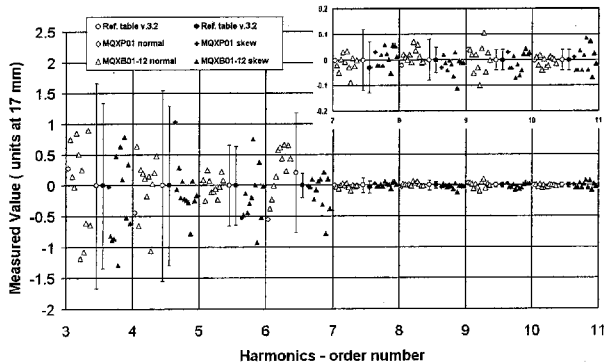


Fig. 5. Integral field harmonics (in units at 17 mm) in MQXB cold masses at 11.9 kA current (214 T/m) compared with the acceptance criteria defined in Ref. Table v.3.2 [3]. The insert shows the higher order harmonics.

TABLE I  
INTEGRAL GRADIENT TRANSFER FUNCTION (T/kA)

Magnet	LHC operation Injection (0.67 kA)	LHC operation Collision (11.9 kA)
LQXB01	202.14 $\pm$ 0.02	197.72 $\pm$ 0.06
LQXB03	202.22 $\pm$ 0.01	197.97 $\pm$ 0.08
LQXB04	202.20 $\pm$ 0.02	197.94 $\pm$ 0.06
LQXB05	202.43 $\pm$ 0.02	197.83 $\pm$ 0.05
LQXB06	202.30 $\pm$ 0.02	198.29 $\pm$ 0.06
Average	202.26 $\pm$ 0.01	197.94 $\pm$ 0.03

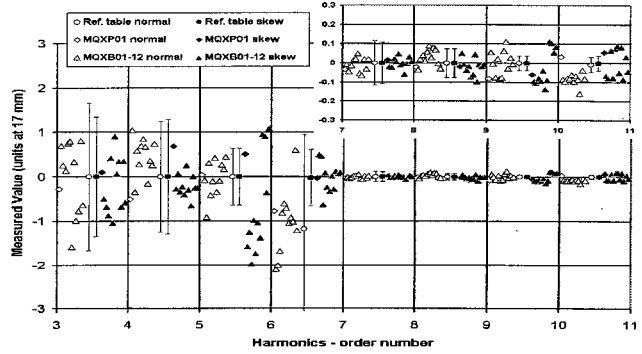


Fig. 6. Integral field harmonics (in units at 17 mm) in MQXB cold masses at 0.67 kA LHC injection current compared with the acceptance criteria defined in Ref. Table v.3.2. The insert shows the higher order harmonics.

standard deviation respectively. One may conclude that at the LHC operating current the low magnet harmonics are within limits. Some of the higher order harmonics ( $b_{9,10}$  and  $a_{9,10}$ ) are outside 3 sigma border. The r.m.s. of the measured central values is in the order of 0.03 units which may point into direction of a possible limitation of the measurement system.

The integral field harmonics at injections current 0.67 kA (12.3 T) is shown in fig.6.

The integral quadrupole gradient transfer function over the 11 m LQXB unit length (one LQXB contains two MQXB cold masses) was measured with SSW and the results are summarized in Table I. The average transfer function is found to be 202.26 $\pm$ 0.01 T/kA at injection (0.67 kA) and 197.94 $\pm$ 0.03 T/kA at collision (11.9 kA).

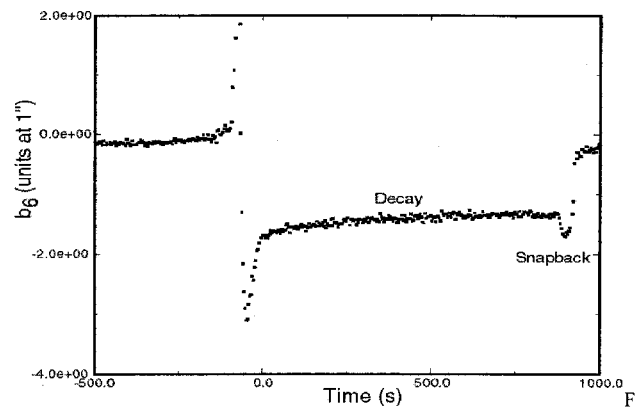


Fig. 7. An example of decay and snap-back of the dodecapole component for a plateau at injection of 900 s in MQXB11.

TABLE II  
DECAY AMPLITUDE AND SNAPBACK TIME IN THE NORMAL DODECAPOLE

Cold mass	Decay Amplitude* (Units at 17 mm)	Decay Time (s)
MQXB01	0.47	12.4
MQXB02	0.34	8.4
MQXB05	0.48	15.9
MQXB06	0.48	14.3
MQXB07	0.28	10.1
MQXB08	0.24	7.9
MQXB09	0.32	9.1
MQXB12	0.33	8.7
Average	0.37	10.1

\* After a subtraction of the underlying hysteresis loop

### C. Decay and snapback

A well-known problem for the superconducting magnets is the decay and subsequent snap back of field components at the injection plateau. To characterize this effect in the MQXB quadrupoles, we performed measurements with an accelerator cycle similar to the one used in the LHC arc dipole tests. The duration of the plateau is 15 min at 0.67 kA (12.3 T/m). Typical example of the decay and snapback in MQXB11 is shown in fig. 7. Table II summarizes the decay amplitude and snapback time for the measured MQXB. The decay and the snapback are parametrized with a logarithmic and gaussian functional forms described in [13]. The average decay amplitude is  $\sim 0.4$  units after 15 min. followed by the snap-back time of  $\sim 10$  s. The MQXB quadrupoles show 4.5 times smaller decay amplitude compared to the LHC arc dipoles for approximately the same injection time [14].

### D. Eddy currents

Current loops at 40 and 80 A/s for MQXB quadrupoles have been executed. The difference between different ramp rate loops was small, indicating small eddy current effects. Table III summarizes the width  $\Delta b_6 = (b_6^{\text{up ramp}} - b_6^{\text{down ramp}})$  of the dodecapole hysteresis at 6.0 kA. The last row in the table averages  $\Delta b_6$  for the model magnets 5 and 9 [3]. One can conclude that MQXB01-12 have a similar behavior to the model magnets and that the Eddy current contribution to  $b_6$  hysteresis is rather small.

## IV. CONCLUSION

Fifteen of a total of eighteen superconducting low-beta quadrupole cold masses for LHC have been produced. The quality assurance warm magnetic measurements after collaring and yoking of these cold masses are within specifications established by the last five short model magnets and the first full scale prototype [3,8,9].

Cold magnetic measurements were performed on the MQXB cold masses assembled in the LQXB cryogenic units. As a whole, at injection and collision, the integral field harmonics are quite small and they are consistent with the reference ones derived from the model magnet program. Some deviations are observed in higher level harmonics (order 9,10) and in the skew decapole at injection.

An additional study of dynamics effects was made at the

TABLE III  
HYSTERESIS WIDTH OF THE DODECAPOLE AT 6.0kA

Cold mass	$\Delta b_6^{40}$ at 40 A/s (Units at 17mm)	$\Delta b_6^{80}$ at 80 A/s (Units at 17mm)	$\Delta b_6^{40} - \Delta b_6^{80}$
MQXB01	-0.60	-0.87	0.27
MQXB02	-0.45	-0.51	0.06
MQXB03	-0.24	-0.38	0.14
MQXB05	-0.28	-0.37	0.09
MQXB06	-0.21	-0.26	0.05
MQXB07	-0.13	-0.35	0.22
MQXB08	-0.19	-0.22	0.03
MQXB09	-0.21	-0.21	0.00
MQXB10	-0.35	-0.35	0.00
MQXB11	0.05	-0.13	0.18
MQXB12	-0.32	-0.42	0.10
Average	-0.27	-0.37	0.10
Model Program	-0.1	-0.35	0.25

injection plateau current. The decay and snap-back after 15min injection showed an average change in  $b_6$  of  $\sim 0.4$  units and consistent decay times of  $\sim 10.1$  s. Eddy current effects leading to large ramp dependence in the allowed harmonics were not observed in the dodecapole hysteresis.

## REFERENCES

- [1] The Large Hadron Collider Conceptual Design, CERN AC/95-05 (LHC).
- [2] T. Ogitsu et al., Status of the LHC Low Beta Insertion Quadrupole Magnet Development at KEK, MT17, CERN, Sep. 2001.
- [3] N. Andreev et al., Field quality in Fermilab-built models of quadrupole magnets for the LHC interaction region, IEEE Trans. Appl. Supercond., Vol. 11, No. 1, March 2001.
- [4] G. Sabbi et al., Correction of High Gradient Quadrupole Harmonics with Magnetic Shims, IEEE Trans. Appl. Supercond., Vol. 10, No. 1, March, 2000.
- [5] R. Bossert et al., Magnetic Measurements of the Fermilab High Gradient Quadrupoles for the LHC Interaction Regions, IEEE Trans. Appl. Supercond., Vol. 9, No. 7, June, 1998.
- [6] N. Andreev et al., Study of Kapton Insulated Superconducting Coils Manufactured for the LHC Inner Triplet Model Magnets at Fermilab, IEEE Trans. Appl. Supercond., Vol. 10, No. 1, March, 2000.
- [7] J. DiMarco et al., Field alignment of quadrupole magnets for the LHC interaction regions, IEEE Trans. Appl. Supercond., Vol. 10, No. 1, March 2000.
- [8] N. Andreev et al., Field Quality in Fermilab-built Models of High Gradient Quadrupole Magnets for the LHC Interaction Region, IEEE Trans. Appl. Supercond., Vol. 10, No. 1, March 2000.
- [9] R. Bossert et al., Field measurement of a Fermilab-built full scale prototype quadrupole magnet for the LHC interaction regions, IEEE Trans. Appl. Supercond., Vol. 12, No. 1, March 2002.
- [10] R. Bossert et al., Field Quality of Fermilab-built Quadrupole Magnets models for the LHC Interaction Region, IEEE Trans. Appl. Supercond., Vol. 13, No. 2, June 2003.
- [11] G. Velez et al., Field Quality of the LHC Inner Triplet Quadrupoles Being Fabricated at Fermilab, PAC 2003, Portland, May 2003.
- [12] Bossert, et al., Test Results from the LQXB Quadrupole Production Program at Fermilab for the LHC Interaction Regions, MT18, Morioka, Oct. 2003.
- [13] G. Velez et al., Measurements of Sextupole Decay and Snapback in Tevatron Dipole Magnets, EPAC 2004, Lucerne, Switzerland, July 2004.
- [14] G. Ambrosio, P. Bauer, L. Bottura, M. Haverkamp, T. Pieloni, S. Sanfilippo and G. Velez, A Universal Scaling Law for the Snapback in Superconducting Accelerator Magnets, These Proceedings.